IEEE Photonics Journal
An IEEE Photonics Society Publication

Open Access

Integrated Optical Chemical Sensor Based on an SOI Ring Resonator Using Phase-Interrogation

Volume 6, Number 5, October 2014

Jin Liu
Xi Zhou
Zhi Qiao
Jianhao Zhang
Chenzhao Zhang
Tuowen Xiang
Lingling Shui
Yaocheng Shi, Member, IEEE
Liu Liu, Member, IEEE

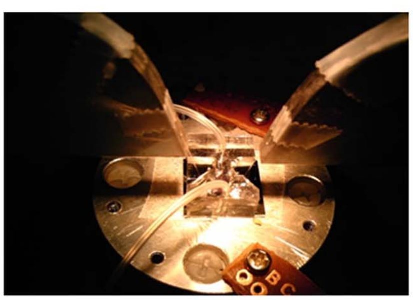

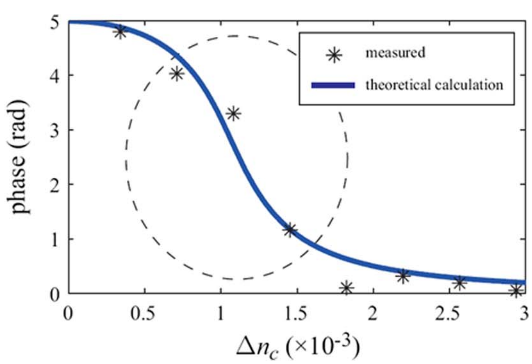

DOI: 10.1109/JPHOT.2014.2352973
1943-0655 © 2014 IEEE

Integrated Optical Chemical Sensor Based on an SOI Ring Resonator Using Phase-Interrogation

Jin Liu,[1] Xi Zhou,[1] Zhi Qiao,[1] Jianhao Zhang,[1,2] Chenzhao Zhang,[1] Tuowen Xiang,[1] Lingling Shui,[3] Yaocheng Shi,[2] *Member, IEEE*, and Liu Liu,[1] *Member, IEEE*

[1]Centre for Optical and Electromagnetic Research, South China Academy of Advanced Optoelectronics, South China Normal University, Higher-Education Mega-Center, Guangzhou 510006, China
[2]Centre for Optical and Electromagnetic Research, Sino-Sweden Joint Research Center of Photonics (JORCEP), Zhejiang Provincial Key Laboratory for Sensing Technologies, Zhejiang University, Hangzhou 310058, China
[3]Institute of Electronic Paper Displays, South China Academy of Advanced Optoelectronics, South China Normal University, Higher-Education Mega-Center, Guangzhou 510006, China

DOI: 10.1109/JPHOT.2014.2352973

Manuscript received July 7, 2014; revised August 15, 2014; accepted August 18, 2014. Date of current version September 9, 2014. This work was supported in part by the National Natural Science Foundation of China under Grant 61107020, Grant 11304102, and Grant 61377023 and in part by the Guangdong Innovative Research Team Program under Grant 201001D0104799318. Corresponding author: L. Liu (e-mail: liu.liu@coer-scnu.org).

Abstract: A phase-interrogation approach for the bulk refractive index sensing based on a silicon-on-insulator (SOI) ring resonator is introduced. The rapid phase variation around the resonance of the ring resonator is interrogated, and a single-sideband generation and coherent detection technology is adopted for the phase measurement. In the proposed approach, most of the intensity noise can be shielded, which leads to an ultra-stable reading for the phase signals. A sensitivity of 6×10^3 rad/RIU and a detection limit of 2.5×10^{-6} RIU are demonstrated.

Index Terms: Silicon-on-insulator, ring resonator, optical sensor, phase interrogation.

1. Introduction

Optical chemical and biologic molecular sensors employing optical resonators and cavities have gained increasing research interests [1]. The basic idea of such sensors is that the effective index of the optical guided mode follows the change of the cladding material due to the evanescent field that leaks into the cladding. In a resonator or cavity structure, this will result in a shift of the resonant wavelength [2]. Recently, silicon photonics and the planar structures based on Complementary-Metal-Oxide-Semiconductor (CMOS) technology have shown their advantages of compact size, low cost, and large-scale integration [3], which leads to successful applications in the field of optical sensing. Micron-sized ring/disk sensing elements and multi-functional integration based on silicon photonics also enable the integration of optical sensors in a lab-on-a-chip system [4].

Conventionally, the wavelength-interrogation or intensity-interrogation is adopted to monitor the responses of a silicon ring or disk resonator [5]. In the first case, a tunable laser source or a

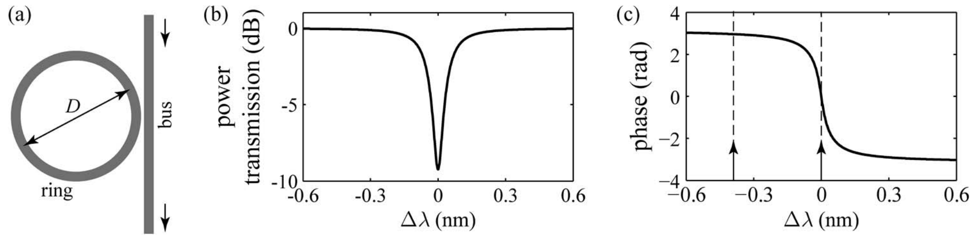

Fig. 1. (a) Schematic plot of a ring resonator side-coupled to one bus waveguide. (b) Power and (c) phase response of the transmitted light around one resonance in the over-coupled regime. The schematic positions of the two laser wavelengths for the phase interrogation measurement are marked with arrows. The following parameters are used here: $r = 0.949$, $a = 0.975$, $n_g = 4.4$, $D = 40$ μm, and $\lambda_r = 1553$ nm.

spectrum analyzer is necessary to measure the wavelength response. With a ring resonator built by silicon-on-insulator (SOI) wire waveguide, a sensitivity of 70 nm/RIU (RIU: refractive index unit) has been demonstrated initially [6], and this figure was lately improved by folds through, e.g., transverse-magnetic (TM) mode excitation, slot waveguide, ultra-small suspended disk, cascaded-ring configuration [7]–[10]. An intensity interrogation approach based on two cascaded SOI rings was also demonstrated using a low-cost broadband source, and a sensitivity of 2×10^4 dB/RIU has been achieved [11]. Besides the sensitivity, detection limit is another important characteristic, which can be defined as, in case of bulk refractive index sensing, the smallest refractive index change that the sensor system can resolve [12]. Normally, the above mentioned wavelength- or intensity-interrogation approaches are vulnerable to noises, such as, alignment accuracy and stability, wavelength scanning accuracy and repeatability, resolution of the spectrum analyzer, etc., which limit the achievable detection limit. Although some of those noise sources can be avoided and a detection limit of 10^{-6}–10^{-7} has been demonstrated, complicated scanning systems and/or carefully designed sensor structures had to be included [12]–[15].

In this paper, a phase-interrogation approach for the bulk refractive index sensing based on an SOI ring resonator is introduced. Various phase-interrogation schemes have been successfully applied to Mach-Zehnder interferometer (MZI) based optical sensors, and shown their abilities to obtain a better detection limit [16] or linearize the readout signals [17]. Here, the rapid phase variation around the resonance of the ring resonator is interrogated, and a single-side-band generation and coherent detection technology is adopted for the phase measurement [18]. In the proposed approach, most of the intensity noise can be shielded, which leads to an ultra-stable reading for the phase signals. A sensitivity of 6×10^3 rad/RIU and a detection limit of 2.5×10^{-6} RIU are demonstrated.

2. Theory and Design

The core sensing element in the proposed phase-interrogation technology is a simple SOI ring resonator side coupled to a straight SOI waveguide, as shown in Fig. 1. The complex transmission coefficient $\tilde{t}$ of the structure around the resonant wavelength can be expressed as [18]

$$\tilde{t} = |\tilde{t}| \exp(j\theta) = \frac{r - ae^{j2\pi n_g \frac{\Delta\lambda}{\lambda_r^2}\pi D}}{1 - rae^{j2\pi n_g \frac{\Delta\lambda}{\lambda_r^2}\pi D}} \quad (1)$$

where r is the amplitude transmission coefficient of the coupling region, a is the round-trip amplitude transmission coefficient along the ring, n_g is group index of the fundamental mode in the SOI waveguide forming the ring, D is the diameter of the ring, λ_r is the resonant wavelength, and $\Delta\lambda$ is the wavelength difference with respect to λ_r.

When the cladding material is changed, the resonant wavelength of the ring shifts correspondingly. This relation can be expressed as [7]

$$\Delta\lambda_r = \lambda_r \frac{\Delta n_{\text{eff}}}{n_g} = \lambda_r \frac{C\Delta n_c}{n_g} \tag{2}$$

where $\Delta\lambda_r$ is the shift of the resonant wavelength, Δn_c is the refractive index change of the cladding material, $\Delta n_{\text{eff}} = C\Delta n_c$ is the corresponding change in the effective index of the waveguide mode, and C is a coefficient related to the waveguide geometry, which can be calculated numerically through, e.g., a waveguide mode solver [19].

Fig. 1(b) and (c) shows the typical power $(|\tilde{t}|^2)$ and phase (θ) transmission spectrum around a resonant wavelength in the over-coupled regime (i.e., $a > r$). In the conventional intensity- or wavelength-interrogation approach, the power transmission coefficient or spectrum is measured, and the resonant wavelength shift is obtained through those data. In the proposed technology, the rapid phase variation around the resonant wavelength is employed. To measure this phase, two laser beams with a certain wavelength spacing are launched together to the bus waveguide. The wavelengths of the two lasers are chosen so that one is align on the resonance of the ring and the other is well off as shown in Fig. 1(c). Once the resonance wavelength of the ring shifts, the phase impinged upon the on-resonance laser changes rapidly, while the phase of the off-resonance one stays almost the same. By measuring the phase difference of these two laser beams transmitted through the ring structure, one can extract the resonance shift, and hence, the refractive index change in the cladding material. In the above approach, the two laser beams share the same light path, and the phase information is adopted. Thus, most power noise sources, such as light coupling instability, measurement setup vibration, etc., can be shielded. This will give ultra-stable readings of the measurement, which will be shown in the following sections. It is also worthwhile to note that operating in the under-coupled regime of the ring resonator gives a non-monotonic phase variation, and thus is not preferable for the sensor application discussed in this paper.

3. Fabrication and Measurement

The designed sensor structures were first fabricated with standard SOI processing technologies, which include 30 keV electron-beam lithography and fluorine-based reactive-ion-etching. A single structure consists of a 40 μm-diameter ring, and two grating couplers for fiber access at transverse-electric (TE) polarization. In order to increase the overlap of the evanescent field to the cladding material, the SOI wire waveguide is chosen to be 350 nm $\times$ 220 nm (width $\times$ height). An array of such structure was prepared with different r by varying the gap between the ring and the bus waveguide, in order to determine the over-coupled regime. Then, an SU-8 layer was spun onto the chip, and openings were fabricated on top of the rings through the layer for analyte access. Finally, a PDMS micro-fluidic channel with a dimension of 100 μm $\times$ 100 μm (width $\times$ height) was attached on the chip for delivering the analyte with the assistance of a syringe pump. During the measurement, the flow rate of the analyte was kept at 25 μl/min. Fig. 2 shows some pictures of the fabricated sample.

The optical measurement setup is sketched in Fig. 3. A single-sideband generation and coherent detection technology is adopted for the phase interrogation. A tunable laser source was first launched to an electro-optical modulator which is driven by a network analyzer at a fixed frequency. The output light consists of two side wavelength peaks and one main wavelength peak with a spacing of the driven frequency. Then, a band pass filter was used to filter out one side peak. The two remaining wavelengths was launched to the chip (which was mounted on a temperature-controlled sample holder) for the measurement purpose. The complex input $\tilde{E}_i(t)$ and output $\tilde{E}_o(t)$ light signals to and from the sensor chip can then be expressed as

$$\tilde{E}_i(t) = \tilde{c}_1 \exp(-j2\pi f_1 t) + \tilde{c}_2 \exp[-j2\pi(f_1 - f_{\text{mod}})t] \tag{3}$$

$$\tilde{E}_o(t) = \tilde{t}_1\tilde{c}_1 \exp(-j2\pi f_1 t) + \tilde{t}_2\tilde{c}_2 \exp[-j2\pi(f_1 - f_{\text{mod}})t] \tag{4}$$

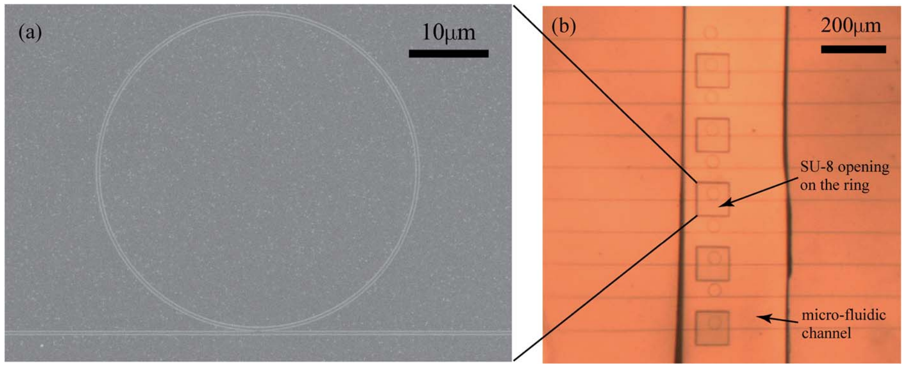

Fig. 2. (a) Scanning electron microscope picture of one fabricated SOI ring resonator. (b) Optical microscope image of one finished sample with the SU-8 opening on the ring and the micro-fluidic channel marked.

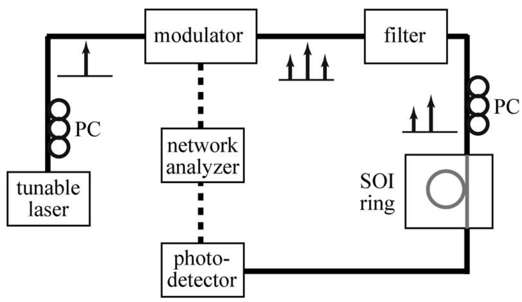

Fig. 3. Optical measurement setup for the phase interrogation. The insets along the light path show the optical spectra at the corresponding positions. PC: polarization controller.

where f_i is the frequency of the input tunable laser, f_{mod} is the driving frequency of the modulator, $\tilde{c}_{1,2} = |\tilde{c}_{1,2}|\exp(j\theta^i_{1,2})$ are the initial complex amplitude of the two laser wavelengths, respectively, which remain constant during the measurement, and $\tilde{t}_{1,2}$ are complex transmission coefficients of the ring at the two laser wavelengths from (1), respectively. The transmitted light was detected by a photo-detector. The output electrical signal reflects the beating wave of the two transmitted laser wavelengths which contains the phase information induced by the ring and can be expressed as

$$I(t) \propto \left|\tilde{E}_o(t)\right|^2 = |\tilde{t}_1\tilde{c}_1| + |\tilde{t}_2\tilde{c}_2| + 2|\tilde{t}_1\tilde{c}_1\tilde{t}_2\tilde{c}_2| \cos[2\pi f_{\text{mod}} t - \Delta\theta^i - \Delta\theta] \tag{5}$$

where $\Delta\theta^i = (\theta^i_1 - \theta^i_2)$, and $\Delta\theta = (\theta_1 - \theta_2)$. The above signal was then fed back to the network analyzer. The network analyzer will automatically filter out the DC component in (5) and extract the phase signal $\Delta\theta^i + \Delta\theta$ (which varies as the resonant wavelength of the ring shifts) in the AC component. Thus, we can monitor the phase induced by the ring directly from the equipment in real time. This insures a very fast sampling frequency for the measurement. We refer to [18] for more details about this coherent detection technique for measuring the phase of the ring.

4. Results and Discussion

NaCl aqua-solutions of different concentrations were used as the analytes. The refractive indices of such solutions have a linear relation to the mass concentration. First, the power transmission spectrum of an over-coupled SOI ring with de-ionized water cladding was measured, as shown in Fig. 4(a). A theoretical fit by (1) is also included. The quality factor (Q, defined as the ratio of the resonance wavelength over the 3-dB bandwidth of the resonance) of the ring is not

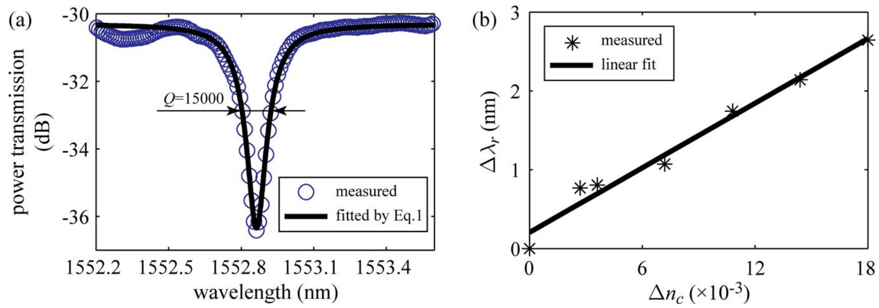

Fig. 4. (a) Power transmission spectrum of an over-coupled SOI ring with de-ionized water cladding. A theoretical fit by (1) is also plotted giving $r = 0.925$ and $a = 0.974$, provided $ng = 4.4$ and $D = 40$ μm. (b) Wavelength shift with respect to the refractive index change of the cladding material.

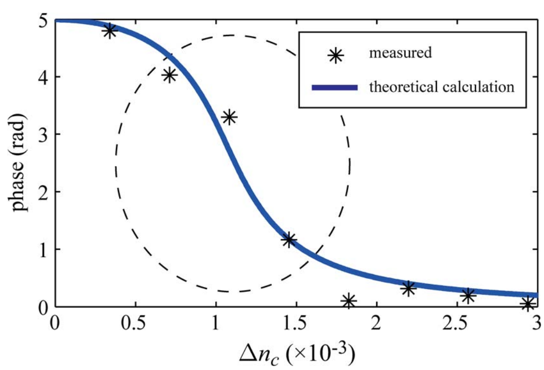

Fig. 5. Theoretically calculated and measured phase from the network analyzer with respect to the refractive index change of the cladding material. The optimal operational regime of the sensor is marked with a dashed ellipse.

very high, i.e., ~15 000, partially due to the un-optimized fabrication technologies. Therefore, for the subsequent phase measurement, the driving frequency of the modulator (cf., Fig. 3) was set to 40 GHz, in order to have the two input laser wavelengths at different resonant conditions of the ring as described in Section 2. The wavelength shift with respect to different concentrations of the analyte solution were first measured, as shown in Fig. 4(b). A linear fit of 136 nm/RIU can be obtained, which is close to the theoretical calculation of 150 nm/RIU for the chosen dimension of the SOI waveguide at TE polarization. If we take the wavelength measurement accuracy to be the wavelength repeatability of the employed tunable laser, i.e., 2pm, the detection limit of this wavelength interrogation can be extracted [12], i.e., 1.47×10^{-5} RIU. Note that this is the best-case estimation. The intensity noise in the transmission spectrum will give rise to a large uncertainty in determining the resonant wavelength of the ring, which will make the detection limit much worse [5].

In the phase interrogation measurement, we initially set the wavelength of the tunable laser longer than the resonant wavelength of the ring in the case of de-ionized water cladding, so that the resonant wavelength can shift across it when the concentration of the analyte increases. The measured phase with respect to the refractive index change of the cladding material is shown in Fig. 5, which matches well to the theoretical calculation based on the parameters derived from Fig. 4(a). The dashed ellipse in Fig. 5 indicates the regime where the phase exhibits a large variation when the refractive index of the cladding material changes, and thus is the optimal working regime for the sensing application. A maximal sensitivity (defined as the first-order differential of the curve shown in Fig. 5) of the present device is 6×10^3 rad/RIU. It is worthwhile to note that the optimal working regime can be shifted towards $\Delta n_c = 0$ by setting the

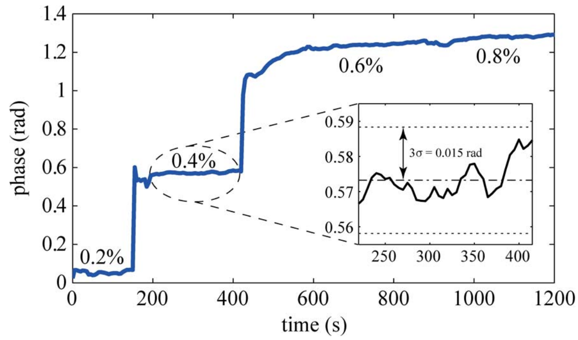

Fig. 6. Continuously measured phase when different concentrations of NaCl solutions flew through the sample. Numbers marked beside various sections of the curve indicate the corresponding mass concentration of the solution being used. The inset shows a zoom-in plot of the section marked with the dashed ellipse. The sampling interval between the data points is 5 sec.

wavelength of the tunable laser close to the resonant wavelength of the ring, so that the maximal sensitivity can be obtained in the beginning of the measurement. The optimal working regime can also be extended by using cascaded ring configuration [21].

To further investigate the stability of the proposed phase-interrogation approach, the phase signal $\Delta\theta$ was continuously sampled by a computer program, while different concentrations of NaCl solutions flew through the sensor structure. The measurement results are shown in Fig. 6. Sudden jumps seen in the curve indicate the moments when the analyte changes. Once the analyte concentration becomes stable, the measured phase signal exhibits a typical 3σ noise of 0.015 rad, as shown in the inset of Fig. 6. Taking the maximal sensitivity of the device discussed above, the detection limit of the proposed approach reaches 2.5×10^{-6} RIU. This is nearly a six-fold improvement as compared to that obtained in the wavelength interrogation approach mentioned above, even in its best case.

5. Conclusion

We have demonstrated an SOI-ring based bulk refractive index sensor using a phase-interrogation approach. A single-sideband generation and coherent detection technology has been employed to measure the phase of the transmitted optical signal around the resonant wavelength of the SOI ring resonator, which exhibits a rapid variation when the cladding material changes. The extra modulator and the coherent detection technology only need to work at a single frequency, and can be integrated on-chip together with the sensing SOI ring [20]. Therefore, the proposed phase interrogation approach is easy to implement and can have a high integration density. A sensitivity of 6×10^3 rad/RIU has been measured. An ultra-stable reading of the phase signals has also been achieved with a 3σ noise of 0.015 rad due to the suppression of the intensity noise. This leads to a detection limit of 2.5×10^{-6} RIU. A better result can be expected by, e.g, improving the Q-factor of the ring, or using a slot waveguide structure. Wavelength multiplexing and more advanced micro-fluidic systems can also be included to address multiple rings with different resonant frequencies, if several chemicals need to be analyzed at the same time.

References

[1] X. Fan *et al.*, “Sensitive optical biosensors for unlabeled targets: A review,” *Anal. Chim. Acta*, vol. 620, no. 1, pp. 8–26, Jul. 2008.
[2] I. M. White and X. Fan, “On the performance quantification of resonant refractive index sensors,” *Opt. Exp.*, vol. 16, no. 2, pp. 1020–1028, Jan. 2008.
[3] W. Bogaerts *et al.*, “Nanophotonic waveguides in silicon-on-insulator fabricated with CMOS technology,” *J. Lightw. Technol.*, vol. 23, no. 1, pp. 401–412, Jan. 2005.
[4] M. C. Estevez, M. Álvarez, and L. M. Lechuga, “Integrated optical devices for lab-on-a-chip biosensing applications,” *Laser Photon. Rev.*, vol. 6, no. 4, pp. 463–487, Jul. 2012.

[5] J. Hu, X. Sun, A. Agarwal, and L. C. Kimerling, “Design guidelines for optical resonator biochemical sensors,” *J. Opt. Soc. Amer. B, Opt. Phys.*, vol. 26, no. 5, pp. 1032–1041, May 2009.
[6] K. De Vos, I. Bartolozzi, E. Schacht, P. Bienstman, and R. Baets, “Silicon-on-insulator microring resonator for sensitive and label-free biosensing,” *Opt. Exp.*, vol. 15, no. 12, pp. 7610–7615, Jun. 2007.
[7] T. Claes *et al.*, “Label-free biosensing with a slot-waveguide-based ring resonator in silicon on insulator,” *IEEE Photon. J.*, vol. 1, no. 3, pp. 197–204, Sep. 2009.
[8] T. Claes, W. Bogaerts, and P. Bienstman, “Experimental characterization of a silicon photonic biosensor consisting of two cascaded ring resonators based on the Vernier-effect and introduction of a curve fitting method for an improved detection limit,” *Opt. Exp.*, vol. 18, no. 22, pp. 22 747–22 761, Oct. 2010.
[9] S. M. Grist *et al.*, “Silicon photonic micro-disk resonators for label-free biosensing,” *Opt. Exp.*, vol. 21, no. 7, pp. 7994–8006, Apr. 2013.
[10] X. Wang *et al.*, “Suspended ultra-small disk resonator on silicon for optical sensing,” *Opt. Lett.*, vol. 38, no. 24, pp. 5405–5408, Dec. 2013.
[11] L. Jin, M. Li, and J.-J. He, “Optical waveguide double-ring sensor using intensity interrogation with low-cost broadband source,” *Opt. Lett.*, vol. 36, no. 7, pp. 1128–1130, Apr. 2011.
[12] M. Iqbal *et al.*, “Label-free biosensor arrays based on silicon ring resonators and high-speed optical scanning instrumentation,” *IEEE J. Sel. Topics Quantum Electron.*, vol. 16, no. 3, pp. 654–661, May 2010.
[13] D.-X. Xu *et al.*, “Label-free biosensor array based on silicon-on-insulator ring resonators addressed using a WDM approach,” *Opt. Lett.*, vol. 35, no. 16, pp. 2771–2773, Aug. 2010.
[14] H. Sohlström, K. B. Gylfason, and D. Hill, “Real-time label-free biosensing with integrated planar waveguide ring resonators,” in *Proc. SPIE Silicon Photon. Photonic Integr. Circuits II*, May 2010, vol. 7719, pp. 77190B-1–77190B-15.
[15] C. Qiu, J. Chen, and Q. Xu, “Ultraprecise measurement of resonance shift for sensing applications,” *Opt. Lett.*, vol. 37, no. 23, pp. 5012–5014, Dec. 2012.
[16] R. Halir, L. Vivien, X. Le Roux, D.-X. Xu, and P. Cheben, “Direct and sensitive phase readout for integrated waveguide sensors,” *IEEE Photon. J.*, vol. 5, no. 4, p. 6800906, Aug. 2013.
[17] S. Dante *et al.*, “All-optical phase modulation for integrated interferometric biosensors,” *Opt. Exp.*, vol. 20, no. 7, pp. 7195–7205, Mar. 2012.
[18] M. Pu *et al.*, “Tunable microwave phase shifter based on silicon-on-insulator microring resonator,” *IEEE Photon. Technol. Lett.*, vol. 22, no. 12, pp. 869–871, Jun. 2010.
[19] *FIMMWAVE/FIMMPROP*, Photon Design Ltd., Oxford, U.K. [Online]. Available: http://www.photond.com
[20] P. Verheyen *et al.*, “Co-integration of Ge detectors and Si modulators in an advanced Si photonics platform,” in *Proc. SPIE, Silicon Photon. Photonic Integr. Circuits III*, Jun. 2012, vol. 8431, pp. 843114-1–843114-8.
[21] M. Pu *et al.*, “Widely tunable microwave phase shifter based on silicon-on-insulator dual-microring resonator,” *Opt. Exp.*, vol. 18, no. 6, pp. 6172–6182, Mar. 2010.